Papers submitted to the Conference "Applications of Physics in Mechanical and Material Engineering"

The Simulation of Light Propagation in Biologically Inspired Micro-Waveguide

M. Dośpiał* and K.M. Gruszka

Department of Physics, Czestochowa University of Technology, Ave. Armii Krajowej 19, 42-200 Czestochowa, Poland

Doi: 10.12693/APhysPolA.142.35 *e-mail: marcin.dospial@pcz.pl

Bee's eye has thousands of integrated optical units called ommatidia. Each ommatidium consists of a light-diffracting facet lens, a crystalline cone, and photoreceptor cells with a wave-guiding rhabdom. The presented work shows the simulation of propagation of light in a biologically inspired micro-waveguide based on the structure of the bee's sensory elements in compound eyes. The propagation was analyzed using the Meep software package for electromagnetics simulation via the finite-difference time-domain method. The transmittance spectra were obtained by the Fourier transform of the response to the short pulse.

topics: finite-difference time-domain (FDTD), waveguide, EM propagation, optical sensors

1. Introduction

The recent development of bio-inspired artificial compound eye (ACE) sensors has a huge potential for wide field-of-view (FOV) imaging and fast motion detection in a miniaturized form [1–6]. Especially the wide FOV exhibits a huge potential for medical, industrial, and military applications.

One of the most interesting biological systems representing application potential in this field is the bee's eye vision system. A natural bee's compound eye consists of a number of sensors called ommatidia, which are used for light detection (Fig. 1a, b) [7]. Every single ommatidium comprises a facet lens, a crystalline cone, a light-guiding rhabdom, and photoreceptor cells (Fig. 1a). A single ommatidium can be anatomically and optically mimicked by self-aligned microlens and optical waveguide (OWG), as shown in Fig. 1c.

In this paper, we present finite-difference time-domain (FDTD) calculation results of short Gaussian type pulse propagation and transmittance spectra in an artificial bio-inspired waveguide for variable entrance angles ranging from 0 up to 32°.

2. Computational methods

For all calculations, we have used the Meep software package [8], which implements the FDTD method for simulating electromagnetic wave propagation. The schematic structure of OWG and referential waveguide (RWG) has been presented in Fig. 2.

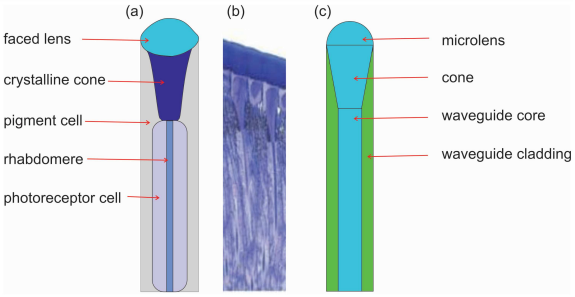

Fig. 1. Schematic of (a) ommatidium in compound eye, (b) fragment of an optical micrograph of a honeybee's apposition compound eye [7], (c) diagram of bio-inspired waveguide.

The models of OWG and RWG used for calculations were composed of two refractive zones, i.e., core and cladding of different ϵ values equal to 2.5 and 1.96, respectively, which corresponds to two types of polydimethylsiloxane (PDMS) polymers [9]. The simulation was made on the basis of lossless materials, therefore the kappa coefficient was not taken into account. In the OWG model, the core zone was placed in the entrance and central zone. Its main components were as follows: microlens with a radius of 1 μm, cone of aperture $D_a = 0.5$ μm, and central core with a length of 10 μm (the calculated Fresnel number F was ranged from 0.029 to 0.055). The core zone in RWG was placed along the waveguide axis in its central part and had a width of 0.5 μm. The cladding zone in

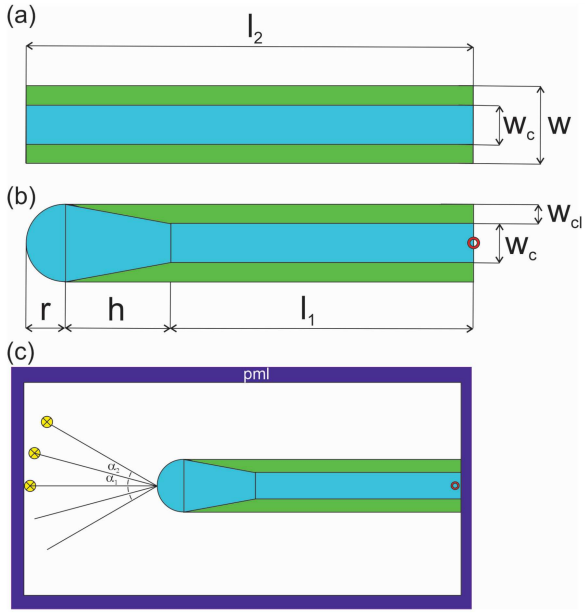

Fig. 2. Diagram of the waveguides structure for RWG (a) and based on the ommatidium OWG (b), where w — core width, w_c — cladding width and aperture diaphragm size, l_1 and l_2 — waveguide lengths, r — lens radius, h — height of crystal cone. (c) The computing domain with arranged elements inside it.

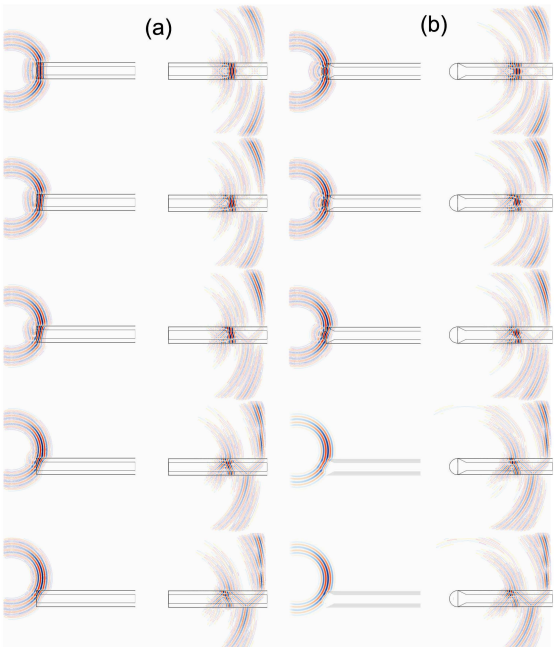

Fig. 3. EM wave propagation in (a) RWG and (b) OWG with different angle of incidence after 17- and 50-time steps.

both types of WG had a width of 0.25 μm. The horizontal length of both waveguides (ACE and RWG) was similar and equal to 12 μm, while their thickness was set to 1.0 μm.

Such prepared waveguide and the light source were placed in the air area surrounded by perfectly matched layers (PMLs) of 1 μm thickness, as can be seen in Fig. 2c.

The light source was placed on the waveguide axis at a distance of 4 μm. In order to determine wave propagation depending on entrance angle, the position of the light source was shifted along an arc of a circle of radius equal to radiation source — waveguide distance in starting position. In the applied simulation, space was digitized. The 50 pixels represented 1 μm of length. Also, in order to reach numerical stability, a 0.5 Courant criterion was used. Based on such assumed variables and the working area, the time step in the simulation was 5 ns.

The Gaussian pulse was set in the transverse electric (TE) mode in such a way that in 2D simulation the E_x and E_y components of the electromagnetic field were parallel to, respectively, the x and y axis of the computational domain. The component E_z was the current component, which was modulated in time. Due to the Meep program using current sources (the electric charge related to J terms in Maxwell's equations), the source used in the simulation was not a hard type of source.

The transmittance spectra were obtained by the Fourier transform of the response to the short pulse. The Fourier transform was calculated at the end of the waveguide just before PML. The calculation was performed along a vector parallel to the waveguide axis at the core center for the area size equal to core width. Obtained waveguide transmittance results were normalized by a similar calculation performed for an empty, air-filled box.

For both types of calculations, a Gaussian-pulse radiation source with 1.67 $[2\pi C/a]$ central frequency and 2.5 $[2\pi C/a]$ width was used, which represents the ultraviolet–visible (UVA-VIS) wavelength area.

3. Results and discussion

In Fig. 3 the electromagnetic (EM) propagation at the entrance and end of waveguides for both RWG and OWG were presented. The red and blue colors represent positive and negative peaks of the E_z component of the electromagnetic field with respect to the surroundings in white, which is treated as zero amplitude. Applied in simulation, EM source generated pulses that have a temporal intensity profile, which has a Gaussian shape. Subjecting such an impulse to a Fourier analysis reveal that different frequencies appear in its spectrum, distributed around the 1.67 $[2\pi C/a]$ central frequency, with a width of distribution equal to 2.5 $[2\pi C/a]$.

The EM wave, regardless of the angle of entry, propagates along the axis of the waveguide. At low angles, the displacement is practically parallel to its

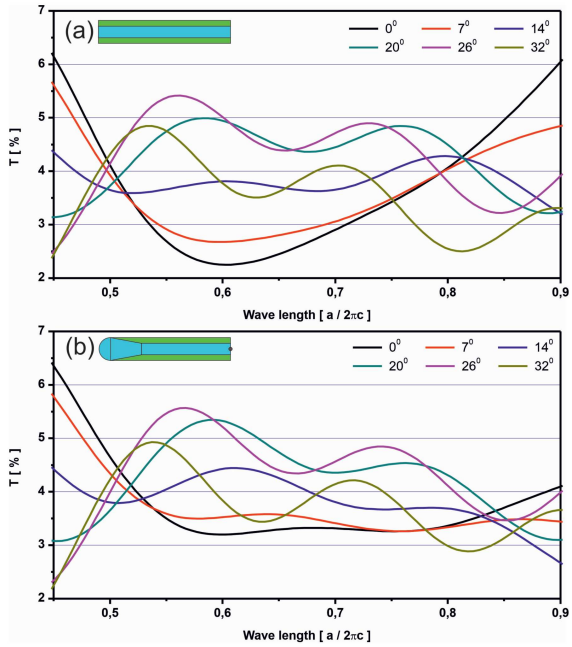

Fig. 4. Transmission spectra for EM wave propagated in (a) RWG and (b) OWG for different angle of incidence.

axis. For higher angles, beam decentration is visible. Lowering the contrast of the wave indicates a gradual decrease in the amplitude of the propagating wave. For high angles, the amplitude decay is faster. In the case of both waveguides, we observe the penetration of part of the wave into the cladding. A faster reduction of wave intensity for a higher angle of incidence should be attributed to more frequent penetration of the wave into the cladding zone of the waveguide. The pulse for the OWG appears to be more focused on the center of the waveguide and slightly more contrasting compared to the RWG. This can be attributed to the greater amplitude of the wave. That, in turn, can be attributed to the change in the direction of light propagation after entering the OWG towards lower angles and thus to a lower frequency of reflections at the boundary of the optic media. As the differences in saturation are difficult to perceive, it was decided to determine the transmission value at the end of the waveguides. This allowed determining not only directional, but also quantitative differences in the propagation of the Gaussian pulse.

In Fig. 4 the transmission spectrum for both waveguides and different angles of incidence were presented. As can be seen, in both waveguides we observe relatively low transmittance values, not exceeding 8% in relation to the reference beam. The transmission trends versus wavelength are similar in both waveguides. In the case of the OWG, one can see an overall (cumulative over all wavelengths) increase in transmittance for each of the angles of incidence. In the case of the smallest discrepancies in the transmittance value (for the highest value of the angle of incidence), its increase, calculated as $(T_{\mathrm{OWG}} - T_{\mathrm{RWG}})/T_{\mathrm{RWG}} \times 100\%$, reached 64%. For the remaining angles, it was higher and exceeded 150%. This allows us to conclude that the OWG has a generally higher transmittance over the entire studied range.

However, it should be noted that although a general increase in the transmittance in the OWG was observed, there are observed wavelengths at low incidence angles where the transmittance of the RWG was equal to or even higher than in the OWG. In the studied range, this was the case for the wavelengths near the infrared. In the case of wavelengths close to the UVA, transmittance changes were not significant. The biggest differences were observed in the VIS area.

4. Conclusions

In this paper, we showed that the bio-inspired waveguide displays better transmission properties than the conventional one (referential). The signal transmitted in the OWG was less blurry and propagated, for higher entry angles of the light beam, along the axis of the waveguide at a smaller angle. This resulted in a change in the amount of reflections inside the waveguide and thus a smaller overall reduction in transmittance.

The overall light transmission for both waveguides was relatively low and did not exceed 8%. The observed changes in transmission in both types of waveguides significantly depended on the wavelength of the pulse and the angle of incidence. There has been a noticeable improvement in transmission, especially in the VIS range, due to the use of a waveguide based on the OWG structure.

The reported parameters suggest that thanks to the applied methodology, by changing the parameters in terms of the Fresnel number and the electric permittivity ϵ of the core and cladding, it is possible to optimize the structure of the waveguide and control the transmission parameters for selected light frequencies.

Acknowledgments

This research was supported in part by PLGrid Infrastructure.

References

[1] L.P. Lee, R. Szema, *Science* **310**, 1148 (2005).

[2] Bo Dai, Liang Zhang, Chenglong Zhao, Hunter Bachman, Ryan Becker, John Mai, Ziao Jiao, Wei Li, Lulu Zheng, Xinjun Wan, Tony Huang, Songlin Zhuang, Dawei Zhang, "Microfluidic-Assisted 3d-Printed Eye (MAP-eye): A Biomimetic Ommatidium Array with Direct Full-Colour 3d to 2d Panoramic Imaging and Position Tracking", preprint (2020).

[3] Huu Phan, Jungho Yi, Joonsung Bae, Hyoungho Ko, Sangmin Lee, Dongil Cho, Jong-Mo Seo, Kyo in Koo, *Micromachines* **12**, 847 (2021).

[4] J. Kim, Ki-Hun Jeong, L.P. Lee, *Opt. Lett.* **30**, 5 (2005).

[5] Hyukjin Jung, Ki-Hun Jeong, *Opt. Express* **17**, 14761 (2009).

[6] Bo Dai, Liang Zhang, Chenglong Zhao, Hunter Bachman, Ryan Becker, John Mai, Ziao Jiao, Wei Li, Lulu Zheng, Xinjun Wan, Tony Jun Huang, Songlin Zhuang, Dawei Zhang, *Nat. Commun.* **12**, 2041 (2021).

[7] K.-H. Jeong, *Science* **312**, 557 (2006).

[8] A.F. Oskooi, D. Roundy, M. Ibanescu, P. Bermel, J.D. Joannopoulos, S.G. Johnson, *Comput. Phys. Commun.* **181**, 687 (2010).

[9] F. Schneider, J. Draheim, R. Kamberger, U. Wallrabe, *Sens. Actuators A: Phys.* **151**, 95 (2009).